Composite Structures 160 (2017) 61–69

Contents lists available at ScienceDirect

Composite Structures

journal homepage: www.elsevier.com/locate/compstruct

Cohesive zone and level set method for simulation of high cycle fatigue delamination in composite materials

Ahmad Amiri-Rad [a,*], Mohammad Mashayekhi [a], Frans P. van der Meer [b]

[a] Department of Mechanical Engineering, Isfahan University of Technology, Isfahan 84156-83111, Iran
[b] Delft University of Technology, Faculty of Civil Engineering and Geosciences, PO Box 5048, 2600 GA Delft, The Netherlands

ARTICLE INFO

Article history:
Received 23 June 2016
Revised 9 August 2016
Accepted 15 October 2016
Available online 17 October 2016

Keywords:
Cohesive zone method
Level set method
Fatigue
Delamination
Fracture mechanics

ABSTRACT

This paper deals with high cycle fatigue delamination in composite materials. The cohesive zone approach along with the level set method is used to simulate fatigue-driven delamination growth. The cohesive zone method is used for calculation of the energy release rate at the crack front because of its superiority over the virtual crack closure technique (VCCT) for bi-material interfaces and non self-similar crack growth. Evolution of the crack front in 3D during fatigue growth is handled with the level set method. The damage variable in the cohesive zone formulation is changed according to the updated level set field. Benchmarks are used to evaluate the performance of the proposed approach in simulation of 3D delamination growth under fatigue loading.

1. Introduction

Delamination is the separation of plies and is one of the most detrimental modes of failure in the composite materials. Delamination can be initiated by cyclic loading, impact, stresses near free edges, manufacturing defects like incomplete wetting or the presence of transverse matrix cracks. Delamination can grow under fatigue loading and lead to reduction of stiffness, lowering of critical buckling load and complete failure of the structure. Accurate modeling of delamination growth under fatigue loading is essential to safe design of composite structures exposed to cyclic loading such as wind turbine blades and aircraft wings.

For the case of small-scale yielding at the crack front, Paris equation has been successfully used to describe crack growth under cyclic loading. First proposed by Paris et al. [1,2], this equation is usually presented in terms of either stress intensity factor or energy release rate:

$$\frac{da}{dN} = C\left(\frac{\Delta G}{G_c}\right)^m \tag{1}$$

where C and m are material parameters which depend on the loading mode, G_c is the critical energy release rate which is also dependent on the mode ratio and ΔG is the cyclic range of energy release rate. The variable a signifies the crack length and N is the number of cycles. Although this equation was initially used for metals, it has been successfully applied to the laminated composites too [3,4].

As it is shown in Eq. (1) the calculation of the range of energy release rate ΔG is required at the crack front. The virtual crack closure technique (VCCT) is often used in metals for calculation of this parameter. However for bi-material interfaces the assumption of linear elasticity leads to oscillatory singular fields at the crack tip. This makes the application of fracture mechanics methods like VCCT far more complex [5]. Moreover VCCT is not very efficient for crack growth analysis, especially in cases with non self-similar crack growth since the elements need to be aligned with the crack front. Remeshing after a step of crack growth is usually required. This makes the simulation process time-consuming and complicates automation.

In this paper, the cohesive zone method is used to calculate the energy release rate. The cohesive zone concept was first introduced by Dugdale [6] and Barenblatt [7] and since then this method has been successfully used to model fracture in adhesive joints [8,9], bi-material interfaces [10,11] and laminated composites [12,13]. In the cohesive zone method, fracture is modeled by use of a non-linear constitutive relation called the traction-separation law. This law provides a relation between the separation of two interfaces and the traction that opposes this separation. If the separation exceeds a limit called the final separation Δ^f, the traction will be reduced to zero and the crack advances. The traction-separation

* Corresponding author.
E-mail address: a.amiririad@me.iut.ac.ir (A. Amiri-Rad).

http://dx.doi.org/10.1016/j.compstruct.2016.10.041
0263-8223/

law is implemented in the finite element framework by use of the interface elements. A more detailed discussion of this model is presented in the next section.

The cohesive zone method has been mainly used for the simulation of crack growth under monotonic loading. Foulk et al. [14] were among the first researchers who extended the cohesive zone method for modeling fatigue crack growth. They achieved this by adding an unloading/reloading path to the Tvergaard's traction-separation law [15]. Several other fatigue models based on the cohesive zone concept have been proposed [16–19]. However these models are more suited for the cycle by cycle analysis and can result in high computational costs in high cycle fatigue simulations.

More recently alternative cohesive zone based models more suited for high cycle fatigue have been proposed by different researchers [20–22]. These models propose phenomenological relations for the growth of the damage parameter in the traction-separation law. As this damage parameter grows, the stiffness of the interface reduces. These damage growth models have some material parameters which need to be determined by means of experiments. Other researchers [23–25] have tried to link the damage growth to the Paris law. This link helps to avoid introduction of additional material parameters apart from the already well known Paris law parameters.

However, there is a difficulty in linking the damage mechanics from a cohesive law to the fracture mechanics of Paris law. In the cohesive law, the energy release rate is defined as the area under the complete traction separation curve. Fatigue cohesive laws have been proposed [23,24], that accelerate damage development based on estimation of the energy release rate. However, during damage development, the final shape of the traction-separation curve and consequently, the energy release rate are yet unknown. Kawashita and Hallett [25] have presented an alternative approach where fatigue degradation is only applied in the element at the crack tip. Upon mesh refinement, this leads to a model where the local fatigue degradation is applied suddenly. A vertical drop in traction is approached. This implies that the complete area under the curve is known at the moment that fatigue damage is applied. For a 2D scenario, where there is a single crack tip element, this works very well. However, in 3D it involves a crack tip tracking algorithm and estimation of the direction of crack propagation.

As an alternative to cohesive zone modeling, Latifi et al. [26] have shown that using a level set approach is very suitable for fatigue analysis. Unlike cohesive laws which deal with local damage development, the level set method deals with velocity of a front, which allows for a direct link with a crack growth rate. In [26], the model is a pure fracture mechanics approach without cohesive zone, but with dedicated element formulation. The model is limited to thin structures and so far only applicable to single delamination. The present paper combines ideas from Kawashita and Hallett [25] and the level set method. The level set method takes care of describing and updating the crack front location, while the cohesive law provides the estimate for the energy release rate. The cohesive law works exactly as the static cohesive law until the level set front passes the integration point. When the front passes an integration point, the damage is set to 1 in that point. This way, a true vertical drop in traction is achieved irrespective of element size.

In the following sections first the basic formulation of the cohesive zone method is presented. Then the level set method and its implementation for triangular elements are reviewed and the proposed approach for simulation of delamination growth is discussed. Finally two benchmark cases are modeled to investigate the performance of the method both in calculation of the energy release rate and in tracking the crack front evolution in 3D.

2. Formulation

2.1. Cohesive zone method

The traction-separation law is implemented in the finite element framework by using the interface elements. Different constitutive formulations have been proposed [11,27–34], among which the bi-linear traction-separation law is the most common one because of its simple shape. In this law an initial stiffness is introduced which ensures the stiff connection between interfaces before the damage initiation. Therefore it contains an initial linear elastic part and a softening part. The shape of the traction-separation law is shown in Fig. 1, where K is the initial stiffness of the interface, T^0 is the strength and G_c is the fracture energy.

In this paper the quasi-static constitutive formulation presented by Turon et al. [28] is used as a starting point. A 3D element with two triangular faces and total number of 6 nodes is implemented in ABAQUS using the user-element subroutine UEL.

The bi-linear traction-separation law can be written as follows:

$$\begin{cases} T_i = K\Delta_i & \text{if } 0 \leqslant \lambda \leqslant \Delta^0 \\ T_i = (1-d)K\Delta_i & \text{if } \Delta^0 \leqslant \lambda \leqslant \Delta^f \\ T_i = 0 & \text{if } \Delta^f \leqslant \lambda \end{cases} \tag{2}$$

where i shows the mode of loading, T is traction, Δ is the separation of interfaces and K is the penalty stiffness. In this equation $\lambda, \Delta^0, \Delta^f$ and d are the equivalent separation, initial separation, final separation and damage in mixed-mode respectively. The equivalent separation λ is the Euclidean norm of the separation components and is calculated as follows:

$$\lambda = \sqrt{\langle \Delta_I \rangle^2 + \Delta_{II}^2 + \Delta_{III}^2} \tag{3}$$

where $\langle\rangle$ is Macaulay brackets. The damage variable d has the following relation with other traction-separation law parameters:

$$d = \frac{\Delta^f(\lambda_{max}^{\tau} - \Delta^0)}{\lambda_{max}^{\tau}(\Delta^f - \Delta^0)} \tag{4}$$

where $\lambda_{max}^{\tau} = \max_{0 \leqslant t \leqslant \tau}\{\lambda(t)\}$ and τ is the time at which d is calculated.

The energy release rate is defined as the total work done per unit area for the complete failure of the material point. This value can be obtained by integrating the complete failure path in the traction-separation response. In the damage models proposed by Turon et al. [23] and Harper and Hallett [24], continuous increase of the damage variable under cyclic loading leads to gradual loss of stiffness in the interface. This increases the separation of the interface as the fatigue damage accumulates which leads to a

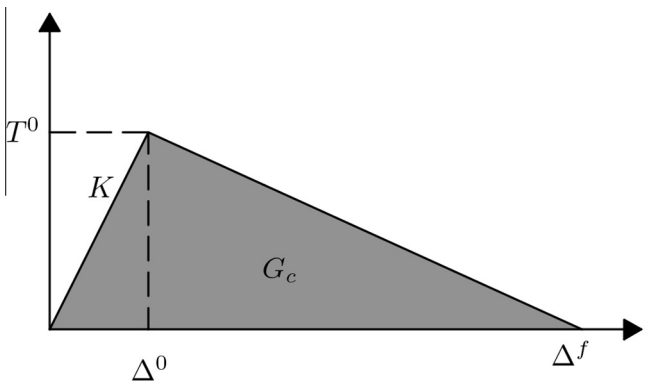

Fig. 1. Bi-linear traction-separation law.

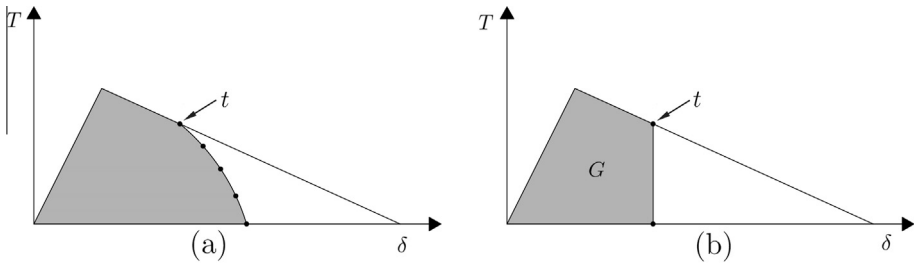

Fig. 2. (a) Non-vertical failure path (b) Vertical failure path.

non-vertical failure path (Fig. 2-a). The non-vertical failure path means the complete failure response and the total dissipated energy would be unknown at the moment t when the crack growth rate is being calculated. Kawashita and Hallett [25] limited the damage accumulation to the element adjacent to the crack tip. As a result the loss of stiffness would happen only to a small part of the interface and the failure path would be close to vertical. In the limit case where the element size at the crack tip goes toward zero, this path becomes completely vertical (Fig. 2-b). In this paper a vertical path is achieved irrespective of the element size by setting the damage variable equal to 1 at nodes which have been passed by a moving front described with the level set method. At the integration points adjacent to the front, the energy release rate is known and can be obtained from the following relation:

$$G = \frac{T^0}{2}\left[\Delta^f - \frac{(\Delta^f - \lambda)^2}{\Delta^f - \Delta^0}\right] \tag{5}$$

The cyclic variation of energy release rate ΔG in Eq. (1) is defined as:

$$\Delta G = G_{max} - G_{min} \tag{6}$$

By using the load ratio R, the cyclic variation of energy release rate ΔG can be computed by using G_{max}:

$$\Delta G = (1 - R^2)G_{max} \tag{7}$$

using Eq. (5), ΔG can be written as follows:

$$\Delta G = \frac{T^0}{2}\left[\Delta^f - \frac{(\Delta^f - \lambda_{max})^2}{\Delta^f - \Delta^0}\right](1 - R^2) \tag{8}$$

For the mixed-mode loading Δ^f and Δ^0 are found using the following relations [28]:

$$\Delta^f = \frac{\Delta_I^0 \Delta_I^f \left(\Delta_{shear}^0 \Delta_{shear}^f - \Delta_I^0 \Delta_I^f\right)\beta^\eta}{\Delta^0} \tag{9}$$

$$\Delta_0 = \sqrt{\left(\Delta_I^0\right)^2\left(\left(\Delta_{shear}^0\right)^2 - \left(\Delta_I^0\right)^2\right)\beta^\eta} \tag{10}$$

where $\Delta_{shear} = \sqrt{\Delta_{II}^2 + \Delta_{III}^2}$ and $G_{shear} = G_{II} + G_{III}$. The parameter η is a material constant which is found by experiment. The variable β is defined as:

$$\beta = \frac{G_{shear}}{G_I + G_{shear}} \tag{11}$$

The fracture energy G_c in mixed-mode loading is described with the relation proposed by Benzeggagh and Kenane [35]:

$$G_c = G_{Ic} + (G_{shear,c} - G_{Ic})\beta^\eta \tag{12}$$

where subscript c is used to show critical energy release rate.

2.2. Level set method

The level set method is a robust tool to track the evolution of moving fronts [36]. In this method the front location is represented by a level set function and as the front moves this function evolves in time. Knowing the velocity at different points of the front, a differential equation for the level set function evolution can be formed [37]:

$$\frac{\partial \varphi}{\partial t} + \nabla\varphi \cdot \boldsymbol{V} = 0 \tag{13}$$

where φ is the level set function and $\boldsymbol{V}$ shows the velocity field. It is beneficial to use a signed distance function as the level set function. The absolute value of the signed distance function at each point shows the shortest distance of that point to the crack front and its sign shows on which side of the crack front the point is located. In the proposed method, the front that is tracked is the crack front that separates the partially damaged cohesive zone from the traction free crack. The positive sign is assigned to the uncracked side and the negative sign to the cracked side (Fig. 3). When φ is a signed distance function, $\nabla\varphi$ is a unit vector and therefore:

$$\nabla\varphi \cdot \boldsymbol{V} = \boldsymbol{V_n} \tag{14}$$

where V_n is velocity value normal to the level sets of φ such as crack front. Using forward Euler time discretization, the level set function φ after time Δt can be found from the following relation [38]:

$$\varphi_{t+\Delta t} = \varphi_t - V_n \Delta t \tag{15}$$

As was discussed in the previous section the energy release rate is calculated at the nodes on the crack front by measuring the area under the traction-separation curves. Since the level set method is used, the crack front is not necessarily aligned with the element boundaries and may pass through the elements. In this case, as shown in Fig. 4, the integration of the traction-separation law will be performed at the nodes of the elements cut by the crack front. A Newton–Cotes integration scheme is used for the cohesive elements which means integration points and nodes are coincident. Therefore values of the energy release rate can be readily calcu-

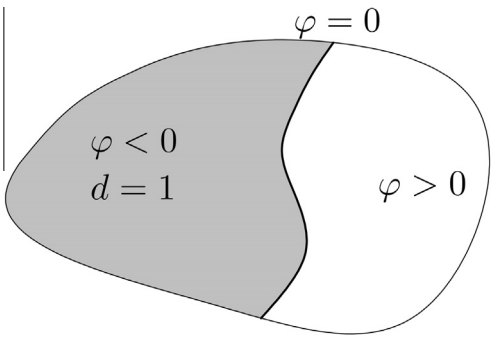

Fig. 3. Signed distance function and damage values in cracked domain.

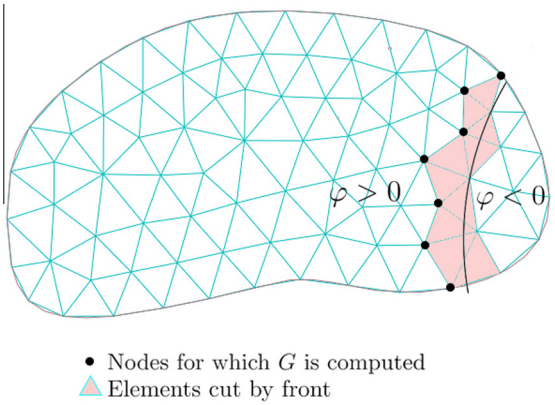

Fig. 4. Calculation of energy release rate at the crack front.

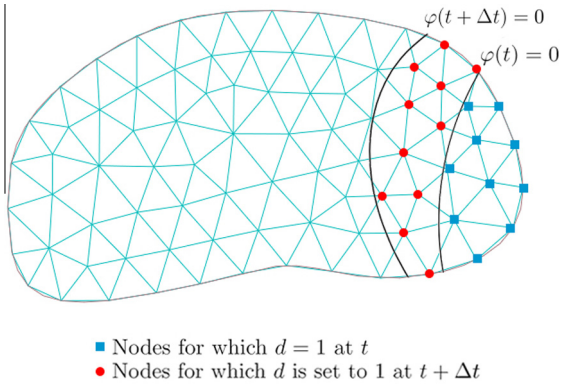

Fig. 5. Change of the damage values at the nodes as the front moves.

lated at nodes. After energy release rate values are obtained, crack growth velocities at these nodes are found using Paris equation (Eq. (1)). The crack growth rate da/dN is used as the velocity V_n required in the level set update equation (Eq. (15)). The time increment Δt in Eq. (15) is actually the number of cycles ΔN in fatigue crack growth. This discretization in time in fatigue problems is called the cycle jump. The cycle jump for any individual time step is chosen using the following equation [23]:

$$\Delta N = \frac{\Delta a_{max}}{\max\left\{\frac{da}{dN}\right\}} \tag{16}$$

where Δa_{max} is maximum amount of crack growth per time step and is pre-established, while $\max\left\{\frac{da}{dN}\right\}$ is the maximum value of the crack growth rate computed along the crack front. Reducing the value of Δa_{max} leads to more accurate results.

For updating the level set function φ, the velocity V_n should be known throughout the domain. Here the fast marching method [37] is used to extend the velocities from the crack front over the whole domain of the interface. The method proposed in [39] is used for extending velocities in triangular elements. In the elements where velocities at two nodes are known, the velocity at the other node is found by solving the normality condition which states that the velocity is constant in the direction normal to the φ level curves:

$$\nabla\varphi \cdot \nabla V_n = 0 \tag{17}$$

If a node is connected to more than one element with known velocities at two nodes, the element which is the most normal to the level set will be used. This is the element with the highest value of $|\nabla\varphi \cdot \nabla N_i|$ where i shows the node with unknown velocity.

While ideally $\varphi_{t+\Delta t}$ will be obtained as a signed distance function, approximation introduced in numerical solution of Eq. (13) will cause deviations. To ensure that the obtained level set function at the next time step $\varphi_{t+\Delta t}$ is a signed-distance function, reinitialization is performed. The reinitialized level set field will have the same zero level curve as $\varphi_{t+\Delta t}$. Reinitialization is performed by solving the equation $|\nabla\varphi| = 1$ by the fast marching method. On a triangular element with two known nodal values, this is a quadratic equation and the root with maximum absolute value will be chosen. If a node is connected to multiple elements, the element with minimum value for $\max\{|\varphi_j|, |\varphi_k|\}$ will be chosen, where j and k are the nodes with known values of φ.

After $\varphi_{t+\Delta t}$ is found, the damage values at the nodes are calculated. For the nodes where $\varphi_{t+\Delta t} < 0$ damage values are set to 1 (Fig. 5). These damage values will be read by the UEL subroutine and therefore the new cracked region will be introduced to the finite element model. The finite element model will be solved again in the next time step with the new crack front and the above described steps will be repeated. The steps of the described procedure are shown in Fig. 6. ABAQUS is used for solving the finite element model. The other tasks in the procedure are performed with a Python code.

3. Results and discussion

In this section a 3D double cantilever specimen and a circular delamination specimen are used to evaluate the performance of the presented approach to simulate fatigue-driven delamination. These two cases are loaded in mode I and mode II respectively. The ability of the method to calculate the energy release rate accurately and to track the crack front is tested.

3.1. 3D double cantilever beam specimen

To investigate the ability of the model to calculate the energy release rate and track the crack front in 3D problems, a double cantilever beam specimen is modeled using cohesive elements. The

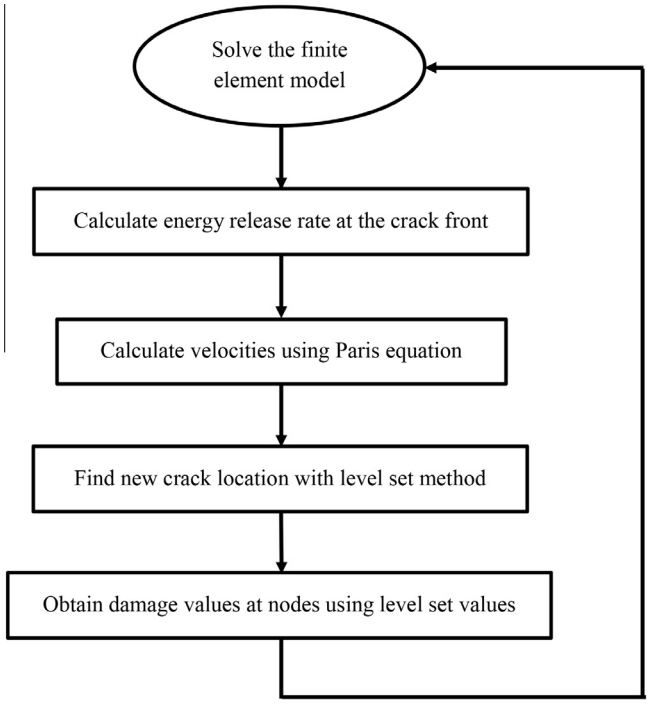

Fig. 6. The steps of crack growth procedure.

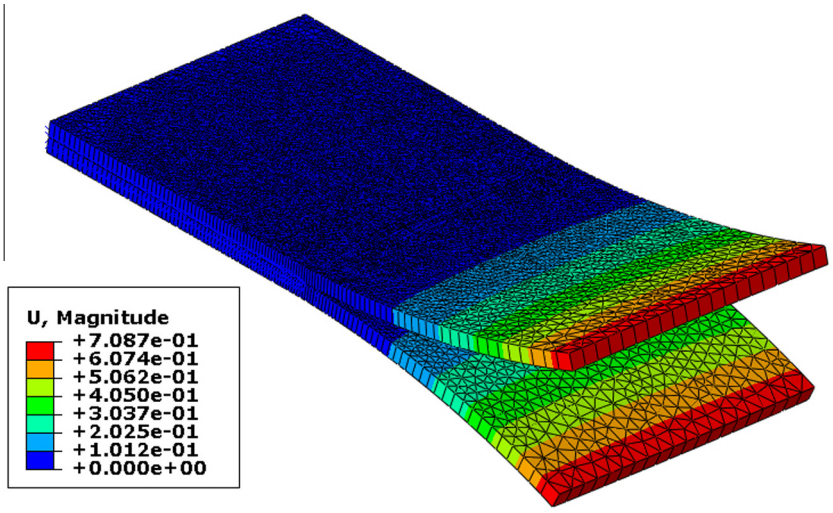

Fig. 7. 3D double cantilever beam specimen.

Table 1
Material properties of HTA/6376C carbon/epoxy [23,40,41].

Elastic constants		Interface properties		Paris Law constants	
E_{11} (GPa)	120	G_{Ic} (kJ/m^2)	0.260	C_I (mm/cycle)	0.0616
$E_{22} = E_{33}$ (GPa)	10.5	G_{IIc} (kJ/m^2)	1.002	m_I	5.4
$G_{12} = G_{13}$ (GPa)	5.25	K (N/mm^3)	10^6	C_{II} (mm/cycle)	2.99
G_{23} (GPa)	3.48	T_I^0 (MPa)	30	m_{II}	4.5
$\nu_{12} = \nu_{13}$	0.3	T_{II}^0 (MPa)	60		
ν_{23}	0.51	η	2.73		

deformed finite element model of the specimen is shown in Fig. 7 with amplified deformations. The specimen has a total length of 20 mm with a delamination length of 10 mm. The specimen width is 10 mm and each arm has a thickness of 0.5 mm. Moments of equal values and opposite directions are applied to each arm while the other end of the specimen is completely fixed. The material properties for HTA/6376C carbon/epoxy are taken from [40,41,23] and shown in Table 1. The laminate is considered to be uni-directional where the fiber orientation is aligned with the beam axis.

The finite element model as shown in Fig. 7 is made from ABAQUS continuum shell wedge elements (SC6R) and the user-defined cohesive elements. Cohesive elements with zero thickness are placed in the delamination plane and a fine mesh with the element size of 0.1 mm is used ahead of the crack front to ensure that the traction distribution in the cohesive zone is captured with good accuracy. The cohesive zone is found as the region ahead of the crack front where damage d has a nonzero value and material points are in the softening zone (Fig. 1).

For the minimum number of elements in the cohesive zone different values have been suggested in the literature. Moës and Belytschko [42] suggested the minimum number of 10 elements in the cohesive zone, while Dávila and Camanho [43] have used 3 elements in their analysis. Because of the small length of the cohesive zone, even using 3 elements in the cohesive zone requires a small element size. Turon et al. [44] have suggested the lowering of the interfacial strength value T^0 to increase the length of the cohesive zone and allow for the bigger elements. However as shown in Fig. 8 too much lowering of the interfacial strength creates problems in capturing the high gradient of G near the free edge. Because of the symmetry the energy release rate distribution on only one half of the front is plotted. In what follows the value of 20 MPa is used for interfacial strength to ensure enough elements exist in the cohesive zone. With this value, the cohesive zone spans approximately 8 elements.

The crack front evolution for 15 steps with $\Delta a_{max} = 0.2$ mm is demonstrated in Fig. 9. To make sure that the accuracy is in an acceptable range, a small value for the step size is chosen. Because of the drop in the energy release rate value near the free edges (Fig. 8) the initial straight line changes to a curved shape. As was discussed in Section 2.2 when the level set function is updated and the new crack front is found, damage values at the integration points with the negative value of the level set function are set to 1 (Fig. 5). This will cause the crack front to fall inside the cut elements and be influenced by the shape of the element boundaries. As a consequence oscillations may occur in the energy release rate values computed at the nodes. These oscillations reduce by mesh refinement and can be removed by applying a smoothing procedure. Here the smoothing is applied each time the finite element model is solved by ABAQUS and the energy release rate is obtained at the nodes of elements that are cut by the front. Oscillations in the energy release rate will be discussed in more detail in the next example.

3.2. Circular delamination specimen

In this section another example is studied to investigate the performance of the presented approach. A circular delamination test with a central crack for mode II delamination is modeled [45]. The position of the circular crack and the boundary conditions are schematically shown in Fig. 10. With the depicted boundary conditions the crack growth will be in mode II only. The specimen has a radius of 20 mm, thickness of 1 mm and the radius of the initial crack is 5 mm. The material of the specimen is HTA/6376C car-

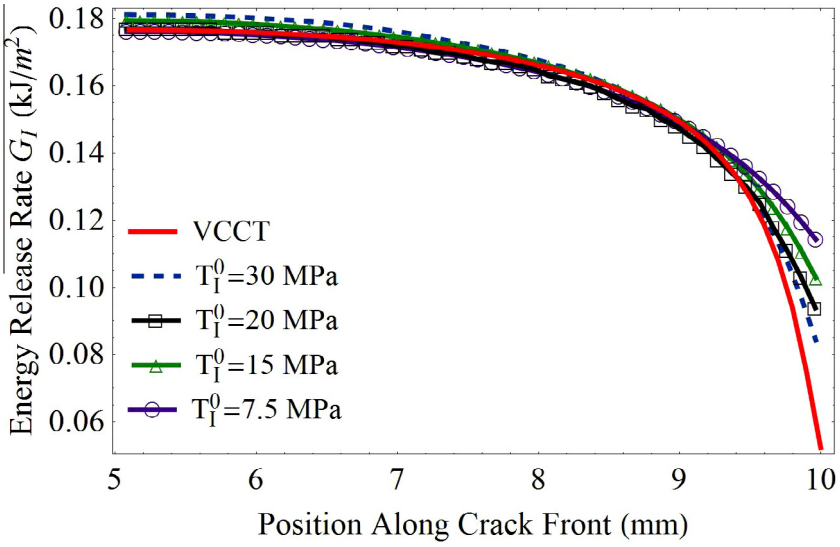

Fig. 8. Energy release rate distribution along initial crack front for DCB specimen for different values of interfacial strength.

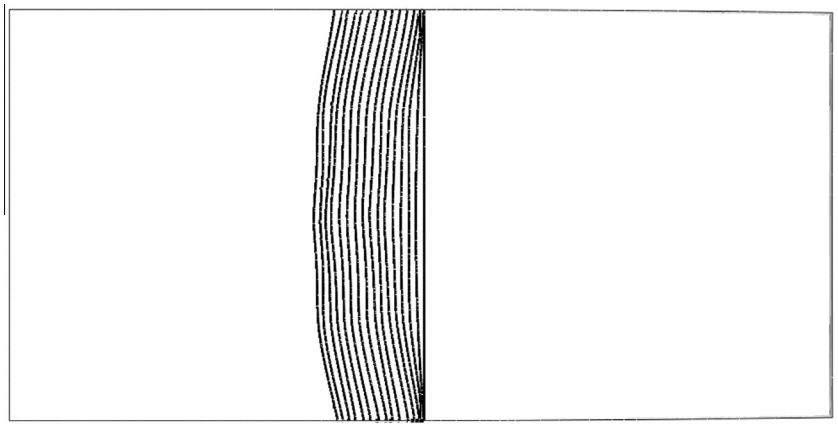

Fig. 9. Evolution of crack front under cyclic loading for DCB specimen.

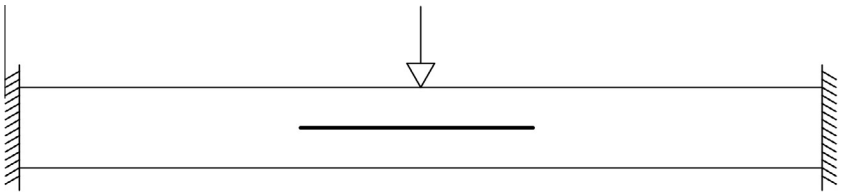

Fig. 10. Circular delamination specimen.

bon/epoxy (Table 1). The laminate is made from two $[-45/90/45/0]_s$ sublaminates. The initial crack is located between the two sublaminates. This layup makes the laminate and the individual sublaminates quasi-isotropic which means that the in-plane material properties can be homogenized. The homogenized properties are shown in Table 2. Paris equation material parameters C and m for mode II are taken equal to 2.99 mm/cycle and 4.5 respectively.

The finite element model constructed for the circular delamination test is shown in Fig. 11. The load applied to the center of the specimen is 400 N. Two rows of the ABAQUS continuum shell wedge elements (SC6R) at above and below the delamination plane are used. These elements follow the first-order shear deformation theory and only have translational degrees of freedom. Between these two rows, one layer of cohesive elements with zero thickness is inserted. Although the model with homogenized laminate properties is axisymmetric and can be reduced to a 2D model, this will not be favorable since the goal here is to investigate 3D crack growth. However symmetry is used to only model a quarter of the specimen. To capture the traction distribution accurately at the crack front, a fine mesh is used. In the initial delaminated area

Table 2
Homogenized material properties of HTA/6376C carbon/epoxy.

E (GPa)	ν	G_{IIc} (kJ/m^2)	T_{II}^0 (MPa)
47.77	0.3	1.002	60

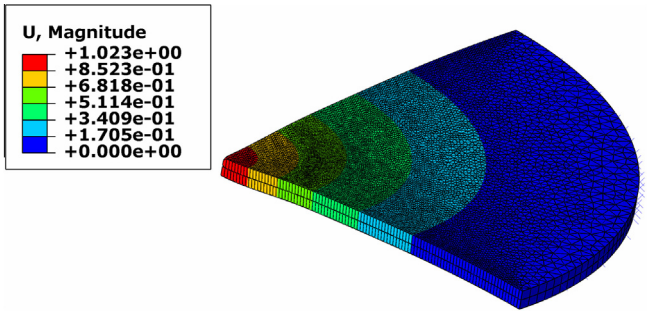

Fig. 11. Finite element model of the circular delamination specimen.

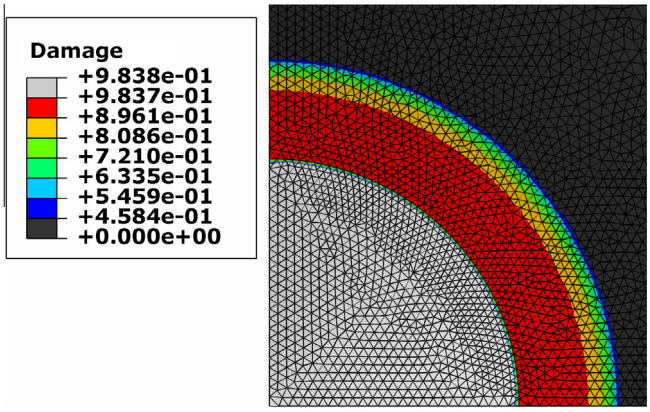

Fig. 12. Cohesive zone ahead of the crack front.

which represents a circle with radius of 5 mm no cohesive elements are used and contact is defined to prevent interpenetration.

As it is shown in the flowchart depicted in Fig. 6 the first step is to solve the finite element model and calculate the energy release rate at the crack front. The cohesive zone obtained from the finite element solution of the model in the first step is shown in Fig. 12.

As shown in Fig. 4, the crack front may pass through elements and is not necessarily aligned with the element boundaries. In the elements that are cut by the crack front the damage value d (Eq. (4)) in the nodes on the cracked sides is set to 1. This will cause the crack front to fall somewhere inside the element and be affected by the shape of the element boundaries. This may create oscillations in the calculated energy release rate values. However by reducing the element size the oscillations will decrease and the solution will improve. Energy release rate values for a circular crack with radius of 10 mm where the crack is no longer aligned with the element boundary are shown in Fig. 13 for two mesh sizes. The angle θ in Fig. 13 is the angle with the x axis which is aligned with the horizontal edge of the specimen in Fig. 12. As it is seen in this figure oscillations have reduced for the smaller mesh size. Besides reducing the element size, smoothing can also be used for alleviating the oscillations. This will be discussed in more detail in the next paragraphs. For obtaining the energy release rate by VCCT a 2D axisymmetric model is made and ABAQUS' own implementation of VCCT is used.

The energy release rate calculation and crack growth for an elliptical crack is also examined. An elliptical crack with major axes of 5 and 10 mm is inserted in the mid-plane of circular delamination specimen. As shown in Fig. 14 good agreement exists between energy release rate values calculated using cohesive elements and values obtained from VCCT. Because for the initial crack, element boundaries are actually aligned with the crack front, the energy release rate curve is smooth and no oscillations are present.

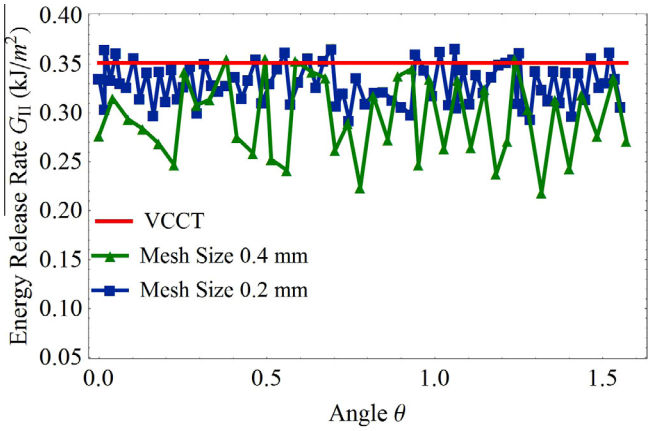

Fig. 13. Energy release rate distribution along crack front.

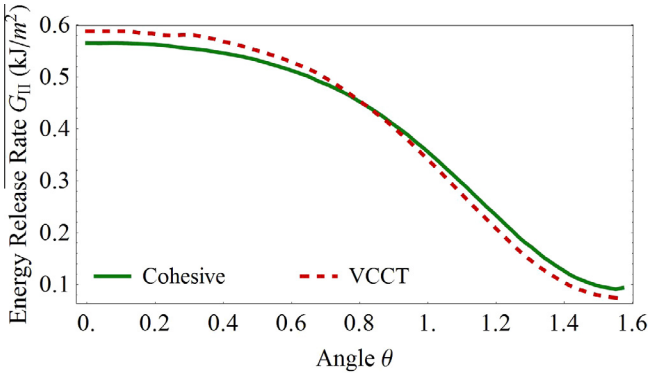

Fig. 14. Energy release rate at crack front.

As it is seen in Fig. 14 the maximum energy release rate value occurs at $\theta = 0$. The size of the cycle jump ΔN is obtained by choosing Δa_{max} equal to 0.3 mm (Eq. (16)). A small value for Δa_{max} is chosen to ensure that the results have acceptable accuracy. The damage values assigned to integration points after 3 steps of crack growth are depicted in Fig. 15. The white area in Fig. 15 shows the initial crack and the red area shows the crack extension. The finite element model is solved using these damage values and energy release rate along the new crack front is calculated. Obtained energy release rate values for this step are plotted in Fig. 16. As

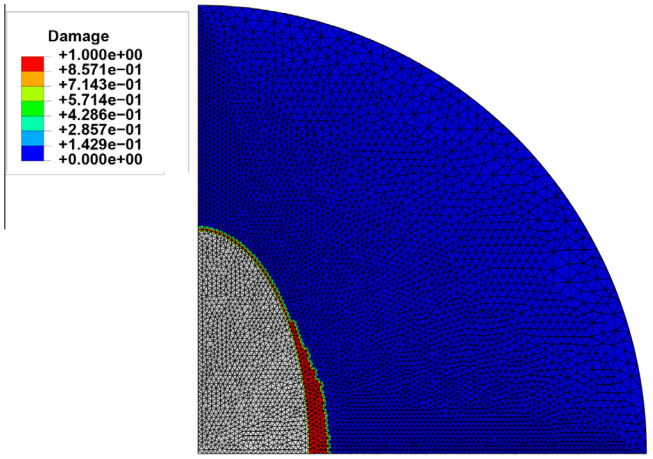

Fig. 15. Damage values assigned to integration points.

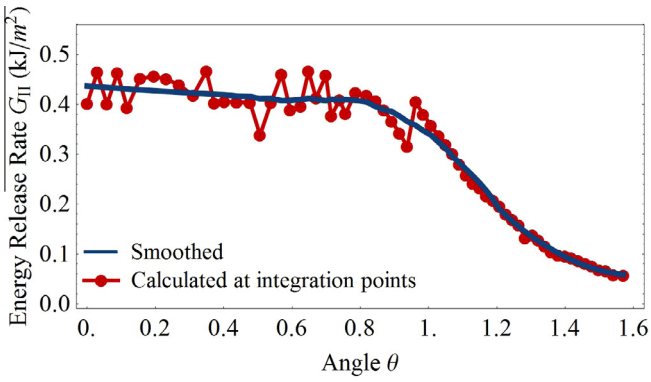

Fig. 16. Energy release rate at crack front.

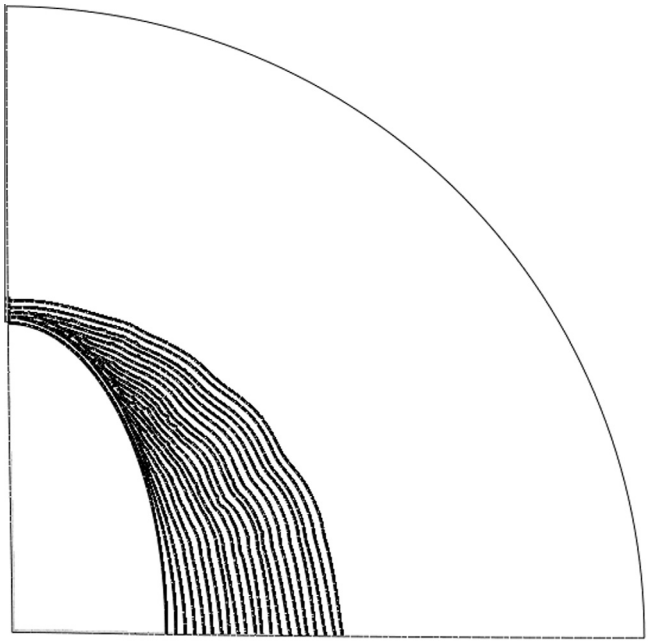

Fig. 17. Crack front evolution.

it is seen in this figure oscillations exist in the energy release rate values. As was discussed earlier the noise can be reduced by refining the mesh but also a smoothing procedure can be applied to remove the oscillations. The smoothed curved is plotted in Fig. 16. Here the Savitzky-Golay filter [46] has been used for smoothing.

As it is observed from Fig. 16 the energy release rate can be obtained accurately by integrating the traction-separation curve at integration points in elements cut by the crack front. The oscillations which occur in the energy release rate calculation can be alleviated by refining the mesh or by applying a smoothing procedure.

The crack front evolution for 20 steps with $\Delta a_{max} = 0.3$ mm is demonstrated in Fig. 17. The initial elliptical crack is expected to grow to a circular shape. As it is seen in Fig. 17 the proposed method tracks the crack evolution to a circular front very well. A slight deviation from a true circle is observed which can be reduced by refining the mesh. As it is seen in Fig. 15 the meshing of the specimen is completely irregular. The presented benchmarks show the ability of the proposed approach to efficiently handle the two main constituents of fatigue crack growth simulations which are the calculation of energy release rates and the tracking of the crack front.

4. Conclusion

A new method is proposed for modeling high cycle fatigue delamination in composite materials. The presented approach is based on a cohesive zone model and uses the level set method for tracking the crack front evolution in 3D problems. The integration of the traction-separation curve at integration points is used to calculate the energy release rate accurately. This method is superior to VCCT since it can be used for bi-material interfaces and no remeshing is required for arbitrary crack growth. Smoothing is proposed to reduce the oscillations of the calculated energy release rates at integration points. Since the velocity at the nodes is required by the level set method, the Newton–Cotes integration scheme is used. Unlike previous fatigue models based on the cohesive zone method, the presented approach does not introduce new material parameters or require calculation of an effective length. The benchmarks show the ability of the method to simulate fatigue-driven delamination and track the front evolution in 3D.

Acknowledgement

The first author would like to thank Iran's National Elites Foundation for their kind support.

References

[1] Paris PC, Gomez MP, Anderson WE. A rational analytic theory of fatigue. Trend Eng 1961;13(1):9–14.
[2] Paris P, Erdogan F. A critical analysis of crack propagation laws. J Basic Eng 1963;85(4):528–33.
[3] Gustafson C-G, Hojo M. Delamination fatigue crack growth in unidirectional graphite/epoxy laminates. J Reinf Plast Compos 1987;6(1):36–52.
[4] O'Brien T. Characterization of delamination onset and growth in a composite laminate. ASTM Spec Tech Publ 1982;775:140–67.
[5] Tzu-Chiang W, Shih CF, Zhigang S. Crack extension and kinking in laminates and bicrystals. Int J Solids Struct 1992;29(3):327–44.
[6] Dugdale D. Yielding of steel sheets containing slits. J Mech Phys Solids 1960;8(2):100–4.
[7] Barenblatt GI. The mathematical theory of equilibrium cracks in brittle fracture. Adv Appl Mech 1962;7(1):55–129.
[8] Blackman B, Hadavinia H, Kinloch A, Williams J. The use of a cohesive zone model to study the fracture of fibre composites and adhesively-bonded joints. Int J Fract 2003;119(1):25–46.
[9] Wei Y, Hutchinson JW. Interface strength, work of adhesion and plasticity in the peel test. Int J Fract 1998;93:315–33.
[10] Tvergaard V, Hutchinson JW. The influence of plasticity on mixed mode interface toughness. J Mech Phys Solids 1993;41(6):1119–35.
[11] Needleman A. A continuum model for void nucleation by inclusion debonding. J Appl Mech 1987;54(3):525–31.
[12] Corigliano A. Formulation, identification and use of interface models in the numerical analysis of composite delamination. Int J Solids Struct 1993;30(20):2779–811.
[13] Schellekens J, De Borst R. On the numerical modelling of edge delamination in composites. Key Eng Mater 1996;120:131–60.
[14] Foulk J, Allen D, Helms K. A model for predicting the damage and environmental degradation dependent life of scs-6/timetal21s [0]4 metal matrix composite. Mech Mater 1998;29(1):53–68.
[15] Tvergaard V. Effect of fibre debonding in a whisker-reinforced metal. Mater Sci Eng, A 1990;125(2):203–13.
[16] De-Andrés A, Pérez J, Ortiz M. Elastoplastic finite element analysis of three-dimensional fatigue crack growth in aluminum shafts subjected to axial loading. Int J Solids Struct 1999;36(15):2231–58.
[17] Yang B, Mall S, Ravi-Chandar K. A cohesive zone model for fatigue crack growth in quasibrittle materials. Int J Solids Struct 2001;38(22):3927–44.
[18] Nguyen O, Repetto E, Ortiz M, Radovitzky R. A cohesive model of fatigue crack growth. Int J Fract 2001;110(4):351–69.
[19] Roe K, Siegmund T. An irreversible cohesive zone model for interface fatigue crack growth simulation. Eng Fract Mech 2003;70(2):209–32.
[20] Robinson P, Galvanetto U, Tumino D, Bellucci G, Violeau D. Numerical simulation of fatigue-driven delamination using interface elements. Int J Numer Methods Eng 2005;63(13):1824–48.
[21] Munoz J, Galvanetto U, Robinson P. On the numerical simulation of fatigue driven delamination with interface elements. Int J Fatigue 2006;28(10):1136–46.

[22] Amiri-Rad A, Mashayekhi M, van der Meer FP, Hadavinia H. A two-scale damage model for high cycle fatigue delamination in laminated composites. Compos Sci Technol 2015;120:32–8.
[23] Turon A, Costa J, Camanho P, Dávila C. Simulation of delamination in composites under high-cycle fatigue. Compos Part A Appl S 2007;38 (11):2270–82.
[24] Harper PW, Hallett SR. A fatigue degradation law for cohesive interface elements–development and application to composite materials. Int J Fatigue 2010;32(11):1774–87.
[25] Kawashita LF, Hallett SR. A crack tip tracking algorithm for cohesive interface element analysis of fatigue delamination propagation in composite materials. Int J Solids Struct 2012;49(21):2898–913.
[26] Latifi M, van der Meer FP, Sluys LJ. A level set model for simulating fatigue-driven delamination in composites. Int J Fatigue 2015;80:434–42.
[27] Camanho PP, Davila C, De Moura M. Numerical simulation of mixed-mode progressive delamination in composite materials. J Compos Mater 2003;37 (16):1415–38.
[28] Turon A, Camanho PP, Costa J, Dávila C. A damage model for the simulation of delamination in advanced composites under variable-mode loading. Mech Mater 2006;38(11):1072–89.
[29] Allix O, Ladeveze P, Corigliano A. Damage analysis of interlaminar fracture specimens. Compos Struct 1995;31(1):61–74.
[30] Allix O, Corigliano A. Modeling and simulation of crack propagation in mixed-modes interlaminar fracture specimens. Int J Fract 1996;77(2):111–40.
[31] Xu X-P, Needleman A. Numerical simulations of fast crack growth in brittle solids. J Mech Phys Solids 1994;42(9):1397–434.
[32] Tvergaard V, Hutchinson JW. The relation between crack growth resistance and fracture process parameters in elastic-plastic solids. J Mech Phys Solids 1992;40(6):1377–97.
[33] Cui W, Wisnom M. A combined stress-based and fracture-mechanics-based model for predicting delamination in composites. Composites 1993;24 (6):467–74.
[34] Schellekens J, De Borst R. A non-linear finite element approach for the analysis of mode-i free edge delamination in composites. Int J Solids Struct 1993;30 (9):1239–53.
[35] Benzeggagh M, Kenane M. Measurement of mixed-mode delamination fracture toughness of unidirectional glass/epoxy composites with mixed-mode bending apparatus. Compos Sci Technol 1996;56(4):439–49. http://dx.doi.org/doi:10.1016/0266-3538(96)00005-X.
[36] Osher S, Sethian JA. Fronts propagating with curvature-dependent speed: algorithms based on Hamilton–Jacobi formulations. J Comput Phys 1988;79 (1):12–49.
[37] Sethian JA. Level set methods and fast marching methods: evolving interfaces in computational geometry, fluid mechanics, computer vision, and materials science, vol. 3. Cambridge University Press; 1999.
[38] Osher S, Fedkiw R. Level set methods and dynamic implicit surfaces, vol. 153. pringer Science & Business Media; 2006.
[39] van der Meer FP, Moës N, Sluys LJ. A level set model for delamination-modeling crack growth without cohesive zone or stress singularity. Eng Fract Mech 2012;79:191–212.
[40] Asp LE, Sjögren A, Greenhalgh ES. Delamination growth and thresholds in a carbon/epoxy composite under fatigue loading. J Compos Tech Res 2001;23 (2):55–68.
[41] Juntti M, Asp LE, Olsson A. Assessment of evaluation methods for the mixed-mode bending test. Int J Numer Methods Eng 1999;21(1):37–48.
[42] Moës N, Belytschko T. Extended finite element method for cohesive crack growth. Eng Fract Mech 2002;69(7):813–33.
[43] Dávila CG, Camanho PP, de Moura MF. Mixed-mode decohesion elements for analyses of progressive delamination. Proceedings of the 42nd AIAA/ASME/ASCE/AHS/ASC Structures, Structural Dynamics and Materials Conference, Seattle, WA, vol. 179.
[44] Turon A, Davila CG, Camanho PP, Costa J. An engineering solution for mesh size effects in the simulation of delamination using cohesive zone models. Eng Fract Mech 2007;74(10):1665–82.
[45] Davies GA. Benchmarks for composite delamination. Hamilton, UK: NAFEMS Ltd.; 2002.
[46] Savitzky A, Golay MJE. Smoothing and differentiation of data by simplified least squares procedures. Anal Chem 1964;36(8):1627–39.